Neuropharmacology 261 (2024) 110178

Contents lists available at ScienceDirect

Neuropharmacology

journal homepage: www.elsevier.com/locate/neuropharm

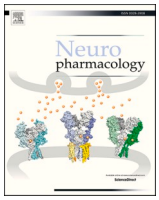

PET imaging identifies anti-inflammatory effects of fluoxetine and a correlation of glucose metabolism during epileptogenesis with chronic seizure frequency

Marion Bankstahl [a,b,c,*], Ina Jahreis [b,d], Bettina J. Wolf [b,d,e], Tobias L. Ross [d], Jens P. Bankstahl [d], Pablo Bascuñana [d,e,f,g]

[a] Department of Laboratory Animal Science and Central Animal Facility, Hannover Medical School, Hannover, Germany
[b] Institute of Pharmacology and Toxicology, University of Veterinary Medicine Hannover, Hannover, Germany
[c] Department of Biological Sciences and Pathobiology, Institute of Pharmacology, University of Veterinary Medicine Vienna, Vienna, Austria
[d] Department of Nuclear Medicine, Hannover Medical School, Hannover, Germany
[e] Institute for Auditory Neuroscience, University Medical Center, Goettingen, Germany
[f] Brain Mapping Unit, Instituto de Investigación Sanitaria Hospital Clínico San Carlos (IdISCC), Madrid, Spain
[g] Department of Nuclear Medicine, Instituto de Investigación Sanitaria Hospital Clínico San Carlos (IdISCC), Madrid, Spain

ARTICLE INFO

Handling Editor: Bruno Frenguelli

Keywords:
Biomarker
Epileptogenesis
Fluoxetine
PET
Serotonin

ABSTRACT

The serotonergic system has shown to be altered during epileptogenesis and in chronic epilepsy, making selective serotonin reuptake inhibitors interesting candidates for antiepileptogenic therapy. In this study, we aimed to evaluate disease-modifying effects of fluoxetine during experimental epileptogenesis.

Status epilepticus (SE) was induced by lithium-pilocarpine, and female rats were treated either with vehicle or fluoxetine over 15 days. Animals were subjected to ^{18}F-FDG (7 days post-SE), ^{18}F-GE180 (15 days post-SE) and ^{18}F-flumazenil positron emission tomography (PET, 21 days post-SE). Uptake (^{18}F-FDG), volume of distribution (^{18}F-GE180) and binding potential (^{18}F-flumazenil) were calculated. In addition, hyperexcitability testing and video-EEG monitoring were performed.

Fluoxetine treatment did not alter brain glucose metabolism. ^{18}F-GE180 PET indicated lower neuroinflammation in the hippocampus of treated animals (−22.6%, $p = 0.042$), but no differences were found in $GABA_A$ receptor density. Video-EEG monitoring did not reveal a treatment effect on seizure frequency. However, independently of the treatment, hippocampal FDG uptake 7 days after SE correlated with seizure frequency during the chronic phase ($r = -0.58$; $p = 0.015$).

Fluoxetine treatment exerted anti-inflammatory effects in rats during epileptogenesis. However, this effect did not alter disease outcome. Importantly, FDG-PET in early epileptogenesis showed biomarker potential as higher glucose metabolism correlated to lower seizure frequency in the chronic phase.

1. Introduction

Epilepsy is one of the most common chronic neurological diseases with more than 50 million affected people worldwide (WHO. Fact sheet epilepsy -http://www.who.int/news-room/fact-sheets/detail/epilepsy). Epilepsy is characterized by an excessive neuronal network activity leading to the occurrence of spontaneous recurrent seizures (Chang and Lowenstein, 2003). The process by which a brain network is functionally altered towards generating spontaneous seizures is called epileptogenesis (Pitkanen et al., 2015). As there is yet no clinically established biomarker to identify patients in risk of developing epilepsy, epileptogenesis is most commonly studied in rodent post-status epilepticus (SE) models (Martín and Pozo, 2006). Using these models, diverse mechanisms have been identified as potential actors in epileptogenesis including altered cerebral glucose metabolism (Jahreis et al., 2021; Zhang et al., 2015), neuroinflammation (Brackhan et al., 2016), neurotransmitter deregulation or neuronal loss (Aronica et al., 2017; Pitkänen and Lukasiuk, 2011).

* Corresponding author. Institute for Laboratory Animal Science and Central Animal Facility, Hannover Medical School, Carl-Neuberg-Str. 1, 30625, Hannover, Germany.
E-mail address: bankstahl.marion@mh-hannover.de (M. Bankstahl).

https://doi.org/10.1016/j.neuropharm.2024.110178
Received 7 August 2024; Received in revised form 1 October 2024; Accepted 3 October 2024
Available online 5 October 2024

Among these, serotonin has shown to be altered both in animal models of epileptogenesis and in chronic epileptic patients. Post-SE rats have shown a decrease of endogenous serotonin concentration in the acute phase of epileptogenesis in two different models using serotonin 1A receptor positron emission tomography (PET) imaging (Bascunana et al., 2019a; Di Liberto et al., 2018; Schönhoff et al., 2021). In addition, serotonin radiotracers have been used to locate epileptic foci in epileptic patients that do not respond to therapy before surgery (Didelot et al., 2008). These observations have encouraged investigations using selective serotonin reuptake inhibitors (SSRIs) as antiepileptic drug in patients (Albano et al., 2006; Neveu et al., 2021) and in animal models (Hernandez et al., 2002; Shiha et al., 2015). In these studies, fluoxetine has shown anticonvulsant effects although the mechanisms are not clear yet. Fluoxetine increases endogenous serotonin concentration by blocking the reuptake system (Stahl, 1998). This increase in serotonin might have anti-convulsant effects by inducing neuronal hyperpolarization (Johnston et al., 2014) through 5-HT_{1A} and/or activating GABAergic interneurons through 5-HT_3 (Stahl, 2015).

On the other hand, anti-epileptogenesis treatments in the clinical setting will only be an option when an identification of the patients at risk is possible. Thus, there is a need of finding biomarkers of epileptogenesis (Pitkanen et al., 2016). These biomarkers need to be non- or minimally invasive (Engel et al., 2013). Nuclear medicine tracers are good candidates due to the low invasiveness of the technique and the existence of small animal scanners for preclinical evaluation, which allows translation of the results. This allows the study of potential imaging biomarkers in animal models using a completely translational method.

The objective of this study was to evaluate the effect of fluoxetine treatment during the acute phase of epileptogenesis in the rat lithium-pilocarpine post-SE model. The antiepileptogenic effect was assessed by video-electroencephalography (video-EEG) monitoring during the chronic phase of this model (12–16 weeks after SE). In addition, we investigated brain glucose metabolism, neuroinflammation and GABAergic neurotransmission during the acute phase and different behavioural comorbidities. Furthermore, we evaluated the biomarker potential of PET imaging with different radiotracers in this model correlating uptake values to the seizure frequency of each animal.

2. Material & methods

2.1. Overall study design and animals

The in vivo experiments performed in this study were performed and are reported in compliance with the ARRIVE 2.0 guidelines (Animal Research: Reporting in Vivo Experiments; Essential 10). The overall design of this study is visualized in Fig. 1.

Female Sprague–Dawley rats (n = 24) purchased from Harlan Italy at a body weight of 200–220 g were housed in pairs in individually ventilated biocontainment units under a 14–10 h light–dark cycle. Cages were equipped with nesting material and environmental enrichment. For video-EEG acquisition, animals were placed individually in specific costume-made cages for two weeks. Standard laboratory chow (Altromin 1324) and water were freely accessible. Before the experiments, animals were allowed to adapt to housing conditions, weighed, marked by the tail, and handled repetitively for at least one week. Experiments were conducted in accordance with European Communities Council Directives 86/609/EEC and 2010/63/EU and were formally approved by the responsible local authority (Niedersächsisches Landesamt für Verbraucherschutz und Lebensmittelsicherheit). All efforts were made to minimize discomfort of the animals.

2.2. SE induction

Unless stated otherwise, all chemicals were of analytic grade and purchased from Sigma-Aldrich. Unsuccessful induction of self-sustaining SE was defined as exclusion criterion *a priori*. SE was induced in female rats (n = 24) of 12–13 weeks of age as described before (Breuer et al., 2017). Briefly, lithium chloride (127 mg/kg, p.o. in 3 ml/kg 0.9% saline) was administered 14–16 h before starting the protocol. First, methyl scopolamine (1 mg/kg, i.p. in 2 ml/kg 0.9% saline) was injected and, after 30 min, pilocarpine administrations were repeated until SE established (30 mg/kg, followed by up to 3 times 10 mg/kg, i.p. in 1 ml/kg 0.9% saline). SE was characterized by the onset of repetitive generalized convulsive seizures (stage 4 or 5)(Racine, 1972) with no recovery of normal behavior. SE was interrupted after 90 min by administration of diazepam (10 mg/kg in 2 ml/kg, i. p.; Ratiopharm). If needed, diazepam injection was repeated up to two times (second repetition, 5 mg/kg) at 15-min intervals. All twenty-four animals developed self-sustaining SE, requiring an average pilocarpine dose of 37.5 ± 7.2 mg/kg. The overall mortality rate was 16.7%, with deaths occurring within the first 48 h after SE. One of the animals died 2 h after SE, before vehicle treatment. After SE, rats were hand-fed with mashed laboratory chow three times per day and received injections of glucose-containing electrolyte solution (Sterofundin HEG-5, B. Braun, Germany; 5 mL s.c.) with a warming pad under the cage until they resumed normal feeding behavior.

2.3. Fluoxetine treatment

The animals were assigned to the treatment groups alternately. This assignment was done before SE induction. Treatment was administered daily (10 mg/kg i.p (Shiha et al., 2015).) for 15 days starting 24 h after SE (n = 12). Fluoxetine hydrochloride was diluted in water for injection (10 mg/kg in 1 ml/kg). Injection solution was prepared freshly before each administration. Vehicle-treated rats (n = 11) were injected with water for injection (1 ml/kg). On days with PET imaging, fluoxetine or vehicle were administered after the imaging protocol to avoid potential bias by acute effects of the drug.

2.4. Radiochemistry

The radiotracer ^{18}F-GE180 was synthesized using a semi-automated module, with high radiochemical purity, yield, and specific activity (450–600 GBq/μmol), as previously described (Thackeray et al., 2018). ^{18}F-FDG was synthesized in clinical grade quality using standard procedures. ^{18}F-FMZ was synthetized as described previously (Kessler et al., 2019). Shortly, F-18 labeling was performed using the corresponding mazenil pinacol borate precursor (5-methyl-6-oxo-8-(4,4,5,

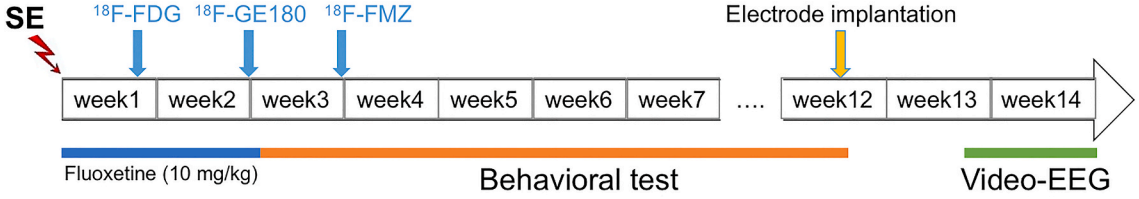

Fig. 1. Timeline of the experimental design. After SE induction as epileptogenesis-inducing insult, animals were treated (fluoxetine or vehicle) for 2 weeks. In addition, they were subjected to PET imaging at week 1, 2 and 3. Behavioral tests for hyperexcitability and anhedonia were performed during the latent phase. Electrode implantation was performed at week 12 and seizure recording (video-EEG) took place during weeks 13 and 14 after SE.

5-tetramethyl-[1,3,2]dioxaborolan-2-yl)-5,6-dihydro-4H-2,5,10b-triazabenzo[e]azulene-3-carboxylic acid ethyl ester, 20 mg) in a Cu (II)-catalyzed (tetrakis(pyridine)copper(II) triflate, 40 mg) F-18 fluorination in N,N-dimethylacetamide (1.0 ml) and a potassium carbonate (0.1 mg) potassium oxalate (1.0 mg) Kryptofix[2.2.2] (6.3 mg) system. Radiosynthesis was automated on a GE TRACERlab® MXFDG in a custom-made cassette system. The crude labeling mixture was then purified on a RP (C18) semi-prep HPLC system using an isocratic eluent of water/acetonitril (75/25) at 3 ml/min flow. The product fraction was isolated and formulated in 0.9% saline (10–15% ethanol) after SPE (C18)-based solvent change.

2.5. PET imaging

At day 7 post-SE, animals were shortly anesthetized using isoflurane (5% for induction, 1–2% for maintenance, regulated depending on breathing frequency, target range of 40–60 breaths per minute) and ^{18}F-FDG (≈20 MBq in 200 μl saline) was injected via the lateral tail vein. Directly after administration, anesthesia was stopped and the rats remained awake for the radiotracer uptake during 25–30 min. Afterwards, rats were again anesthetized by isoflurane and placed in an animal PET camera (Inveon PET scanner, Siemens, Knoxville, USA) with the brain in the center of the field of view, and a 30-min static acquisition scan was performed. Animals were warmed throughout the imaging procedures. Eyes were protected from drying out with a dexpanthenol-containing eye ointment (Bepanthen Nasen-und Augensalbe, Bayer AG, Leverkusen, Germany) and respiration rate was controlled (BioVet software, m2m Imaging, Cleveland, OH, USA) to monitor and, if necessary, adjust depth of anesthesia during the scanning time.

At days 14 and 21 after SE, animals were subjected to dynamic PET scans. First, rats were anesthetized by isoflurane as stated above and a lateral tail vein was cannulated. Then, they were positioned in the PET scanner, the dynamic acquisition (60 min for ^{18}F-GE180 (Wolf et al., 2020) and 45 min for ^{18}F-FMZ (Kessler et al., 2019)) was started and, 10 s later, the radiotracer was injected through the cannula (18.7 ± 0.7 MBq ^{18}F-GE180 or 17.4 ± 1.3 MBq ^{18}F-FMZ in 200 μl saline). At the end of each PET acquisition, a low-dose CT image in the same position was obtained. As supportive measure, rats received an s.c. injection of electrolyte solution (~5 ml, Sterofundin) at the end of PET imaging. They were allowed to recover from anesthesia in a separate, warmed cage before being placed back into their home cages.

For image reconstruction, an iterative ordered subset expectation maximization three-dimensional/maximum posteriori (OSEM3D/fastMAP) algorithm with decay, random, scatter, and transmission corrections was applied.

2.6. Image analysis

After reconstruction, PET images were analyzed by an experimenter blinded to the treatment of each animal fusing them to a brain MRI template (Schiffer et al., 2006) using Pmod software (PMOD 3.7, Zürich, Switzerland). First, PET images were fused to their corresponding CT image and the transformation saved. Separately, CT images were manually co-registered to the MRI template and the transformation saved. Finally, PET images were co-registered to the template and a map of pre-defined regions of interest (ROIs) was applied for quantification. ^{18}F-FDG images were quantified as percent injected dose per gram tissue (%ID/cc). ^{18}F-GE180 images were analyzed calculating the volume of distribution (V_t) of the tracer using a 2-tissue compartment model using an image-derived input function from the carotids as whole-blood activity. No metabolite correction was performed as this approach was highly reliable and correlated to histology (Wolf et al., 2020). On the other hand, ^{18}F-FMZ binding potential (BPnd) was calculated applying the simplified reference tissue model with pons as reference region. In addition, parametric images for each tracer were obtained by statistical parametric comparisons (SPM12, University College London). For voxel-wise comparison, images were compared at group level with a *t*-test using SPM12 with a minimum cluster size of 100 voxels without correction for multiple comparison. In addition, correlation of PET imaging with seizure frequency was performed in SPM12. Uptake quantification of regions that correlated with seizure frequency in SPM12 was graphed.

2.7. Hyperexcitability tests

Assessment of hyperexcitable behavior was performed at weeks one and two post-SE as previously described (Bankstahl et al., 2012). Animal excitability was assessed in the rats' home cages in four tests: approach response, touch response, loud noise reaction, and pick-up. In the approach-response test, a pen hold vertically was moved slowly toward the face of the animal. Responses were scored as: 1 (no reaction), 2 (sniffing at the pen), 3 (moving away from the pen), 4 (freezing), 5 (jumping away from the pen), and 6 (attacking the pen). In the touch-response test, the animal was gently touched on the side with the pen. Responses were scored as: 1 (no reaction), 2 (turning toward the pen), 3 (moving forward, away from the pen), 4 (freezing), 5 (jerking around toward the pen), 6 (turning away from the pen), and 7 (jumping). In the loud noise test, a clicking noise was generated with a clicker, several centimeters above the head of the animal without the animal seeing it. Responses to the noise were scored as the following: 1 (no reaction), 2 (jumping slightly, flinching, or flicking the ears), and 3 (jumping abruptly). In the pick-up test, the animal was picked up grasping it around the body. Responses were scored as: 1 (very easy), 2 (easy with vocalization), 3 (some difficulty, with the rat rearing and facing the experimenter's hand), 4 (freezing), 5 (difficult, the rat moving away), and 6 (very difficult, the rat behaving defensively and/or attacking the experimenter's hand). The behavioral hyperexcitability test was repeated four times by four different blinded experimenters on the same day at 1 h intervals. Order of the animals was randomized to avoid bias. Median scores were used for the subsequent data analysis.

2.8. Sucrose consumption test

During week 5 after SE, sucrose consumption test (SCT) was performed with a sucrose concentration of 1% in drinking water. Rats were separated in individual cages and provided with two tap-water-filled bottles placed on both sides of the cage grid. To rule out a general change in fluid consumption after SE, tap water consumption (using two bottles of water per cage) was measured for 48 h at the beginning of the SCT. During the next 24 h, one bottle was replaced by a bottle containing 1% sucrose. After a 24-h break with both bottles water-filled, the other bottle was replaced by a bottle containing sweetened fluid. Bottles were weighed before and after each 24-h test period to quantify fluid consumption. Consumed amounts of water or sucrose in gram were determined by calculating the mean consumption of the two 24-h test periods. Preference was calculated as the percentage of sweetened solution of total fluid consumption. The person measuring the consumption and changing the bottles was blinded to the treatment of each animal. Animals had free access to food during the whole test.

2.9. Electrode implantation and seizure monitoring

At week 12, animals were subjected to stereotactic surgery for the implantation of hippocampal electrodes. To avoid bacterial infections, animals were treated with marbofloxacin (2 mg/kg, s.c. twice daily, Marbocyl FD 1%, Vetoquinol GmbH, Ravensburg, Germany) for 7 days starting two days before surgery. Briefly, after induction of general anesthesia with isoflurane and positioning in a stereotactic frame (Stoelting), 2% tetracaine hydrochloride solution was applied for local anesthesia of the skin. The skull was exposed and 0.25% bupivacaine hydrochloride (Carbostesin®, AstraZeneca, GmbH, Wedel, Germany)

applied for local anesthesia. A bipolar stainless steel electrode was positioned at the right CA1 region at bregma AP -3.9 mm, LL –1.7 mm, DV -3.5 mm (Paxinos and Watson, 2004) and fixed to the skull using dental acrylic cement (Paladur®, Heraeus Kulzer GmbH, Hanau, Germany). A screw placed over the posterior cortex served as grounding. Three additional screws and dental acrylic cement were used to fix the headset on the skull.

After a week of recovery, animals were placed individually in custom-made clear plexiglass cages for video-EEG recordings by a combined EEG-/video-system similar as previously described (Polascheck et al., 2010). For recording EEG data via LabChart 6 software (ADInstruments, Spechbach, Germany), custom-made cables were coupled to the animal's headsets and to one-channel amplifiers (Bio-Amp, Axon Instruments, Inc. Foster City, CA), which were connected to 8- or 16-channel analogue-digital converters (PowerLab/800s, ADInstruments Ltd., Hastings, East Sussex, UK). The sampling rate was set to 200 Hz and a high pass filter for 0.1 Hz and a Notch-Filter for 50 Hz were applied. Rats were simultaneously video-monitored using light-sensitive black-white cameras (Nycto Systems, Hannover, Germany; 4 to 8 rats per camera). For this purpose, cages were illuminated overnight by infrared diodes. Each animal was recorded 24 h/7 d for 2 weeks, only being disconnected from the EEG for routine measures (cage cleaning, measuring body weight) or to change the cable in case of loss or disturbance of EEG signal. Animals that lost their headset before video-EEG recording was completed (4 rats) were discarded from the statistical analysis for seizure frequency. A total of 17 animals (8 vehicle- and 9 fluoxetine-treated rats) were continuously monitored. The whole EEG data was visually analyzed for paroxysmal events (defined as high-frequency synchronized firing with an amplitude of at least twice the EEG baseline and a duration of at least 8 s) by an experienced researcher not fully blinded to the treatment verifying each event by assessing the animal behavior in the corresponding video recording according to Racine's scale (Racine, 1972). Additionally, all seizures observed during daily handling were noted and classified.

2.10. Statistics

The data is shown as mean ± standard deviation (SD) or median with 95% confidence interval (non-parametric analysis). Data was analyzed with GraphPad Prism7 software (GraphPad Software, La Jolla, CA, USA) using Student's t or Mann-Whitney tests (according to population normality) comparing fluoxetine-treated animals to vehicle-treated rats. A p-value <0.05 was considered statistically significant. Required minimal group size, based on expected variances and differences, was estimated by power analysis ($n = 6$; G*Power, Kiel University, Germany; two-tailed unpaired *t*-test, power: 0.8, α-error: 0.05, effect size: 2.0). The primary outcome measure for group size calculation was ^{18}F-FDG uptake. Additional animals were included to account for the potential dropout rate at any point of the experiment. Mortality rate in both experimental groups were statistically compared (https://www.medcalc.org/calc/rate_comparison.php).

3. Results

3.1. SE

All the 24 rats of this study reached SE, requiring an average pilocarpine dose of 37.5 ± 7.2 mg/kg. Within the first 72 h after SE, four animals died (mortality rate 16.7%) despite our supportive measures. Three of these animals were part of the vehicle group (3/12) and one animal died before receiving any treatment. None of the animals treated with fluoxetine died in the acute phase (0/11). No statistically significant difference but a trend was found in mortality rate between both groups, being lower in fluoxetine-treated animals (95% CI: −0.046 to 0.546; $p = 0.097$).

3.2. PET imaging

In previous experiments, ^{18}F-FDG PET has shown altered brain uptake in the acute phase of this model (Bascuñana et al., 2018; Garcia-Garcia et al., 2017; Goffin et al., 2009; Jahreis et al., 2021). At 7 days after SE, ^{18}F-FDG scans showed no differences between experimental groups in any of the brain ROIs in the atlas-based analysis (Fig. 2A–B). In agreement, statistical parametric mapping showed no significantly different voxels when comparing fluoxetine-with vehicle-treated animals (Fig. 2C).

To assess neuroinflammation, we performed ^{18}F-GE180 scans at 2 weeks post-SE. We observed a decreased tracer V_t in the hippocampus of fluoxetine-treated animals in comparison to the control group ($t(16) = 2.211$; 2.4 ± 0.4 vs 3.1 ± 0.5, $p = 0.042$; Fig. 2D–E). In addition, SPM analysis confirmed the reduction in the hippocampus and showed decreased uptake in sub-regions of the cortex and the amygdala (Fig. 2F).

Due to the effects of serotonin on GABAergic neurons (Stahl, 2015) and as we observed a lasting reduction of ^{18}F-FMZ signal following SE in this animal model (Bascunana et al., 2019b), we investigated the $GABA_A$ receptors during epileptogenesis at 3 weeks after SE. ^{18}F-FMZ imaging revealed no significant BPnd difference between the groups in any of the ROIs selected (Fig. 2G–H). On the other hand, SPM analysis showed small clusters of differences in tracer binding, with increased binding in cortical sub-regions and a decrease in amygdaloid nuclei and areas corresponding to corpus callosum (Fig. 2I).

3.3. Behavior

The antidepressant fluoxetine is a SSRI used also as a treatment for various psychiatric comorbidities in epilepsy. Thus, we evaluated behavioral changes in both experimental groups. Here, we assessed potential changes in behavioral excitability and anhedonia, being indicative of depression-like behavior. Hyperexcitability test showed no differences between experimental groups at one or two weeks after SE (Fig. 3A–B). Similarly, we observed no treatment effect on depression-like behavior, showing comparable preference for sucrose-containing water in both groups (Fig. 3C).

3.4. Seizure frequency

Animals were subjected to video-EEG recordings for two weeks starting at week 13 after SE. Seizure analysis revealed high variability in seizure frequency in both groups (Fig. 3D), but consistent seizure severity (stage 5 of Racine's scale). Statistical comparison showed no significant difference between vehicle- and fluoxetine-treated animals (3.15 vs 0.61; $U = 24.0$; $p = 0.28$).

3.5. PET – seizure frequency correlation

To evaluate the biomarker potential of each tracer used here, we calculated the correlation of these tracers with the seizure frequency in each animal. To this aim, we used parametric images obtained in Pmod software and calculated pixel-wise regression to seizure frequency.

^{18}F-FDG uptake showed the best correlation to seizure frequency of all tracers. Parametric image shows several correlating clusters, being most prominent bilaterally in the dorsal hippocampus (Fig. 4A). Regression calculated with the average hippocampal uptake and seizure frequency shows a negative correlation between both variables ($r(15) = -0.58$, $p = 0.015$; Fig. 4A–B).

On the other hand, parametric regression with ^{18}F-GE180 and ^{18}F-FMZ showed only very limited significant clusters. ^{18}F-GE180 V_t showed a small cluster located in entorhinal cortex (Fig. 4C). However, atlas-based region average plotted against seizure frequency showed no significant correlation between both variables ($r(15) = -0.37$, $p = 0.14$; Fig. 4D) in this region. ^{18}F-FMZ BPnd showed only a weak positive

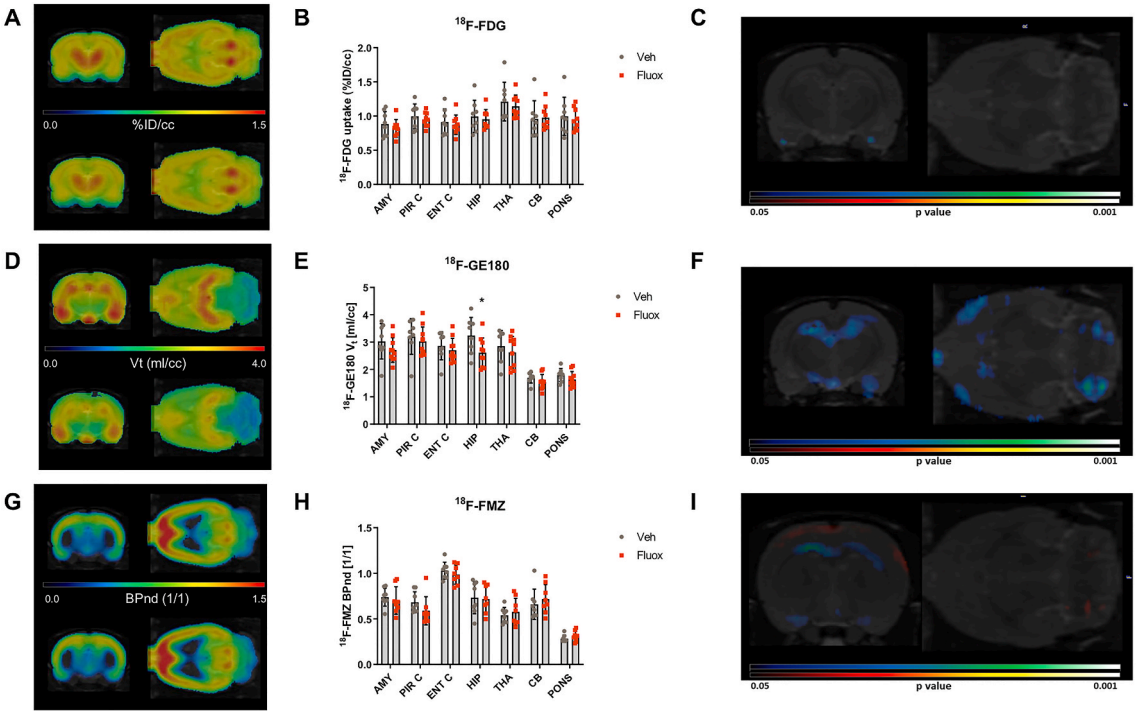

Fig. 2. PET imaging comparison between vehicle- and fluoxetine-treated animals. A, D, and E show average brain images of vehicle- (upper image) and fluoxetine-treated (lower image) rats. ^{18}F-FDG uptake shows no significant differences between both groups (A–C). On the other hand, fluoxetine treatment reduced TSPO expression represented by ^{18}F-GE180 hippocampus V_t both in ROIs (D–E) and voxel-wise analysis (F). Lastly, ^{18}F-FMZ BPnd showed no differences in regional analysis (G–H), but limited alterations in cortical subregions in SPM analysis (I). Data shown as mean ± SD. *$p < 0.05$. Average PET images are shown in cold scale. Parametric maps show significant t values in blue-green (lower uptake/binding) and hot (higher uptake/binding) scale adjusted to a lower threshold corresponding to $p = 0.05$. %ID/cc, percentage injected dose; V_t, volume of distribution, BPnd, binding potential; AMY, amygdala; PIR C, piriform cortex; ENT C, entorhinal cortex; HIP, hippocampus; THA, thalamus; CB, cerebellum; Veh, vehicle; Fluox, fluoxetine.

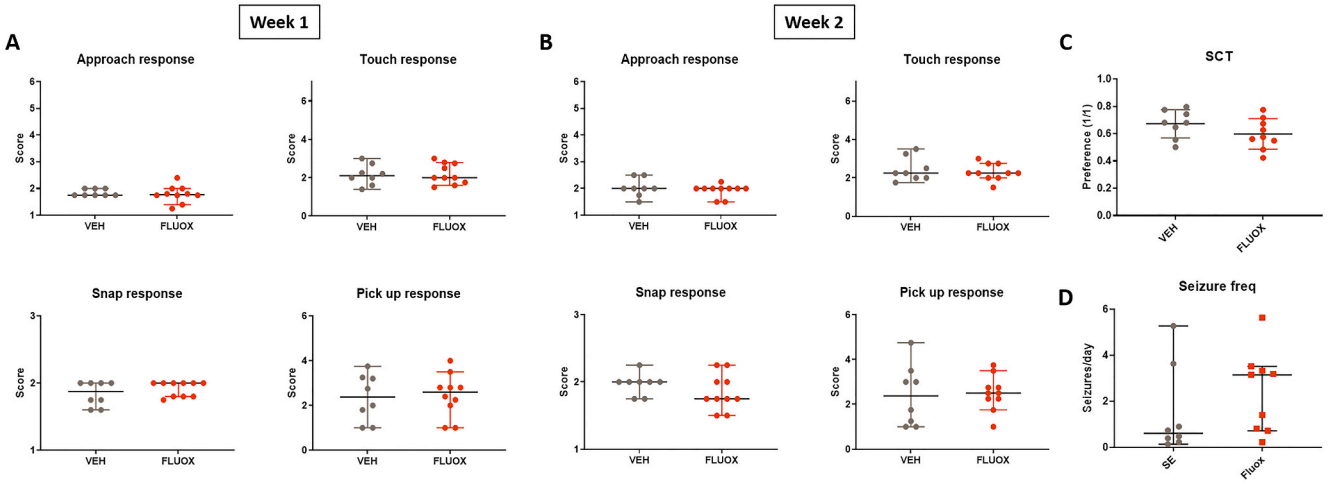

Fig. 3. Behavioral and video-EEG analysis. Hyperexcitability tests showed no effect of fluoxetine treatment on hyperexcitability in any of the time points investigated (A–B). Similarly, at 5 weeks post SE, sucrose-consumption test (SCT) did not reveal any impact of fluoxetine treatment on sweetened fluid consumption (C). Seizure frequency resulting from two weeks of video-EEG analysis in the chronic disease phase shows high variation in both groups with no significant difference (D). Data shown as median with 95% confidence interval except for sucrose consumption (mean ± SD). VEH, vehicle; FLUOX, fluoxetine; freq, frequency.

correlation trend to seizure outcome in sub-regions of the ventral hippocampus ($r(14) = 0.45$, $p = 0.08$; Fig. 4E–F).

4. Discussion

In this study we evaluated the potential anti-epileptogenic effect of fluoxetine when administered in the acute phase of epileptogenesis for two weeks after SE. PET imaging revealed anti-inflammatory effect of fluoxetine. However, video-EEG monitoring showed no change in seizure frequency in fluoxetine-treated animals in comparison to controls. On the other hand, parametric analysis of PET images showed a negative correlation between ^{18}F-FDG uptake 1 week after SE and seizure frequency in the chronic phase of the model.

Fluoxetine is an anti-depressant drug that has previously shown anticonvulsant effects in patients (Albano et al., 2006; Neveu et al., 2021) and animal models of epilepsy (Hernandez et al., 2002; Watanabe

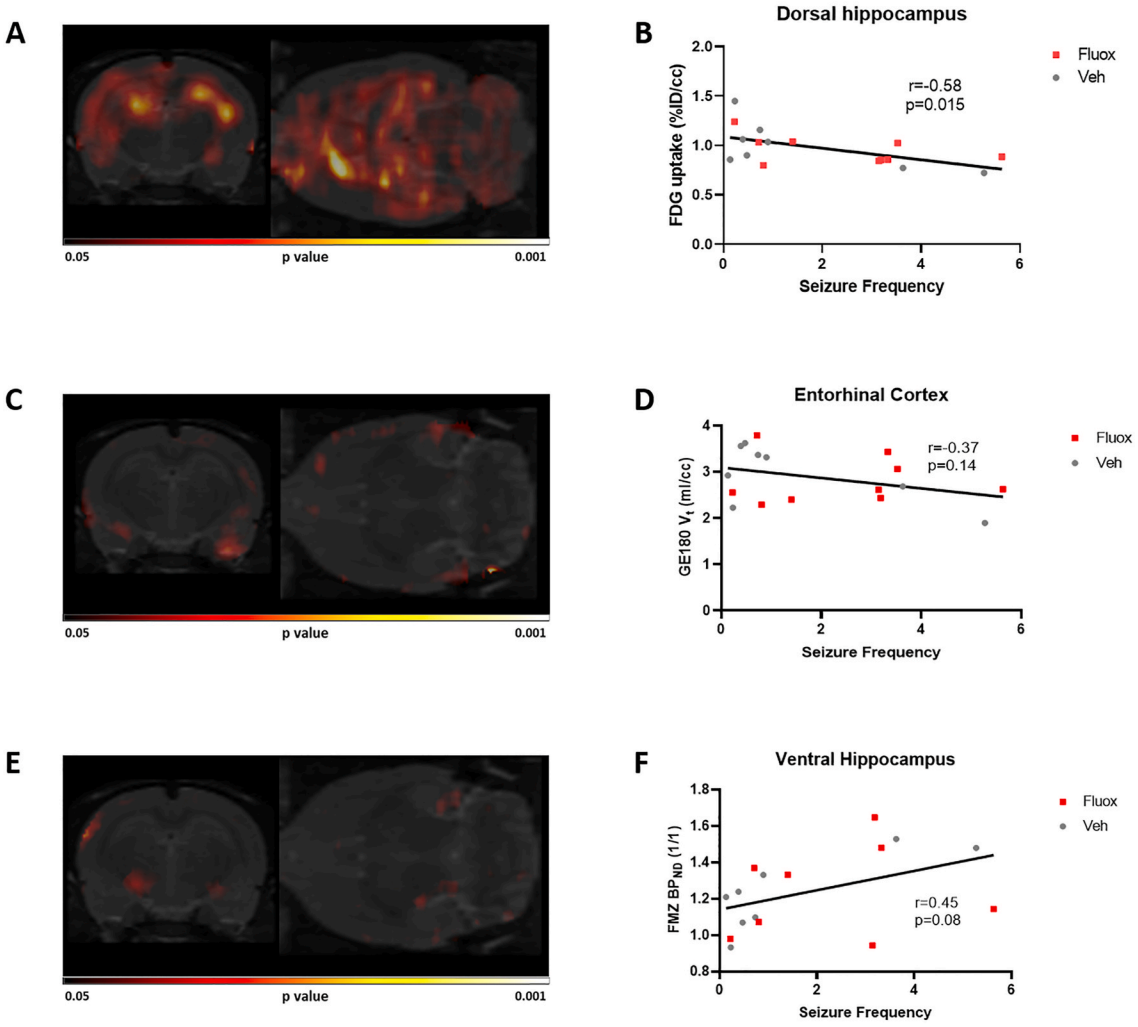

Fig. 4. Correlation between brain glucose metabolism (^{18}F-FDG PET), neuroinflammation (^{18}F-GE180 PET), and $GABA_A$ receptor density (^{18}F-FMZ PET) during epileptogenesis and seizure frequency in chronic epileptic rats. ^{18}F-FDG uptake at one week after SE shows a strong correlation with the most prominent cluster in hippocampus (A). Average hippocampal uptake correlates with seizure frequency (B). On the other hand, ^{18}F-GE180 V_t at two weeks (C–D) and ^{18}F-FMZ BPnd at three weeks after SE (E–F) show no significant correlation to seizure frequency. Parametric maps show significant t values in hot scale adjusted to a lower threshold corresponding to $p = 0.05$. Veh, vehicle; Fluox, fluoxetine.

et al., 1998; Yan et al., 1995) and status epilepticus (Shiha et al., 2015). However, it is not clear how fluoxetine reduces hyperexcitability in these models. Fluoxetine increases endogenous serotonin concentration in the synaptic cleft by blocking the reuptake system (Stahl, 1998). This increase in serotonin might have anticonvulsant effects through different serotonin receptors such as 5-HT_{1A} and 5-HT_3. The 5-HT_{1A} receptor is present in pyramidal neurons, and its activation induces neuronal hyperpolarization (Johnston et al., 2014), while 5-HT_3 is expressed in GABAergic interneurons. Serotonin binding to 5-HT_3 receptors leads to inhibition of cortical pyramidal neurons due to activation of GABAergic inhibition(Stahl, 2015). In addition, fluoxetine alters other neurotransmitters (Bymaster et al., 2002; Koch et al., 2002) as well and there are serotonin receptors in other brain cells (Azmitia et al., 1996) that should not be ignored as a potential source of the anticonvulsant effect of this drug. Thus, we here aimed to evaluate its potential disease-modifying effect on epileptogenesis.

We did not find any changes in brain glucometabolism due to fluoxetine treatment using ^{18}F-FDG PET imaging. In a previous study, it was shown that a 7-day pre-treatment with fluoxetine before SE can partially prevent the hypometabolism in the latent phase described in this animal model (Shiha et al., 2015). Fluoxetine pre-treatment also reduces SE severity and, therefore, probably also the hypometabolism associated to it. However, when applied after the SE, fluoxetine is not altering glucose brain uptake. Thus, the effect previously observed might be due to the anticonvulsant effect of fluoxetine during SE, i.e., a modification of the epileptogenesis-inducing brain insult. On the other hand, ^{18}F-GE180 did show a reduction of the volume of distribution in animals treated with fluoxetine. This effect was also reported when fluoxetine was administered before the SE (Shiha et al., 2015). However, pathways or mechanisms involved in this anti-inflammatory effect are not completely understood. It has been proposed that fluoxetine inhibits microglial activation regulating the Notch and NF-κB pathway or the levels of BDNF (Petry et al., 2023; Yao et al., 2023; Zhang et al., 2022). Although it has been shown that fluoxetine can activate GABAergic neurons through 5-HT_3 receptors (Stahl, 2015), no significant differences were detected in ^{18}F-FMZ PET between experimental groups. GABAergic PET imaging was performed 3 weeks after SE, i.e., one week after finishing the treatment. It might be that the effect of the treatment had subsided at the imaging time point or that the activation through $5HT_3$ does not induce a significant increase in benzodiazepine receptors.

As fluoxetine is an anti-depressant drug, we performed a series of behavioral tests to evaluate potential changes in hyperexcitability and depression-like behavior with the treatment. None of these tests showed any difference between groups. Although fluoxetine is a widely-used

anti-depressant drug, we saw no effect on depression-like behavior in our model. It has been previously shown that lithium-pilocarpine rats do not respond to anti-depressive treatment with fluoxetine in the chronic phase of the disease(Mazarati et al., 2008). However, in both studies, fluoxetine treatment was administered weeks before the SCT to investigate its anti-epileptogenic effect, which could explain the lack of effect. As a final outcome measure of a potential disease-modifying effect of fluoxetine, we measured seizure frequency in the chronic phase of the model (13–15 weeks after SE). We found high variability of seizure frequency in both experimental groups that lead to no statistical difference. Thus, fluoxetine showed no anti-epileptogenic effect in the lithium-pilocarpine model suggesting that the effects seen previously in this model (Hernandez et al., 2002; Shiha et al., 2015) are strictly anticonvulsant but cannot alter the progression of the epileptogenic process. Various studies have suggested that microglial activation might be a key process during epileptogenesis (Bertoglio et al., 2021; Vezzani et al., 2011, 2013). Thus, we performed TSPO-PET imaging to evaluate the effect on microglial activation in fluoxetine- and vehicle-treated animals. PET image analysis showed reduced neuroinflammation in hippocampus, cortex, and amygdala. Fluoxetine treatment has, therefore, an anti-inflammatory effect when administered during the acute phase of epileptogenesis. However, the reduction in neuroinflammation with this treatment has not changed the epileptogenesis process concerning seizure outcome.

To evaluate the biomarker potential of PET imaging with different radiotracers, we correlated seizure frequency to voxel values using SPM software. We found a clear negative correlation between FDG uptake and seizure outcome, being strongest in the dorsal hippocampus. Animals with higher glucose metabolism in the acute phase of epileptogenesis showed lower seizure frequency in the chronic phase, 12 weeks after PET imaging. FDG has previously shown prognostic value in another model of epileptogenesis (Bascuñana et al., 2016) as well as in other neurodegenerative diseases (Blazhenets et al., 2019; Caminiti et al., 2018). Together with these studies, our results suggest that brain glucose metabolism could have a biomarker value for epileptogenesis. Thus, targeting glucose metabolism might be another promising therapy strategy. On the other hand, SPM showed a light correlation between neuroinflammation in entorhinal cortex at two weeks post SE and the final outcome. Other groups have previously reported predictive value for TSPO PET in rat models of temporal lobe epilepsy performed at the same time point as in this study (Bertoglio et al., 2017, 2021; Russmann et al., 2017). However, in our study, TSPO PET showed no strong correlation to seizure frequency. This difference to previous reports might be due to differences among animal models of epileptogenesis or variables studied (frequency groups vs actual seizure frequency). Lastly, FMZ showed a non-significant positive correlation to the occurrence of spontaneous seizures the ventral hippocampus. Thus, animals with higher FMZ binding showed higher seizure frequency. This might reflect an increase in this receptor density or a decrease of endogenous GABA (Bascunana et al., 2019b).

There are some limitations to consider in this study. First, we have only used female rats for this study as they have previously shown lower mortality after lithium-pilocarpine induced SE. Due to the lack of anti-epileptogenic effect of the treatment, further experiments using male rats were discarded. In addition, no *in vitro* assessment of neuroinflammation was performed to confirm imaging results as we have previously demonstrated a clear correlation between histology and TSPO imaging outcome (Brackhan et al., 2016; Wolf et al., 2020). Other tracers targeting synaptic vesicle protein 2A or astrocytes could be of strong interest for future biomarker studies. However, tracer availability limited the inclusion of these in the present study.

In conclusion, this study showed that fluoxetine treatment during epileptogenesis can reduce neuroinflammation but does not alter brain metabolism or $GABA_A$ receptor expression. However, the anti-inflammatory properties did not have an effect on seizure outcome or depression-like behavior. Importantly, FDG PET at an early time point has shown again predictive value in epileptogenesis. Animals with higher FDG uptake in hippocampus have shown a better outcome after epileptogenesis, e.g., lower seizure frequency.

CRediT authorship contribution statement

Marion Bankstahl: Writing – review & editing, Writing – original draft, Methodology, Investigation, Formal analysis, Data curation, Conceptualization. **Ina Jahreis:** Writing – review & editing, Investigation. **Bettina J. Wolf:** Writing – review & editing, Investigation. **Tobias L. Ross:** Writing – review & editing, Investigation. **Jens P. Bankstahl:** Writing – review & editing, Writing – original draft, Supervision, Methodology, Formal analysis, Data curation, Conceptualization. **Pablo Bascuñana:** Writing – review & editing, Writing – original draft, Visualization, Project administration, Investigation, Funding acquisition, Formal analysis, Data curation, Conceptualization.

Declaration of competing interest

The authors declare that they have no known competing financial interests or personal relationships that could have appeared to influence the work reported in this paper.

Data availability

Data will be made available on request.

Acknowledgements

This study was funded by an internal grant from Hannover Medical School ("HiLF"). P. Bascuñana position was funded by the European Seventh's Framework Programme (FP7/2007–2013) under grant agreement n°602102 (EPITARGET). B. J. Wolf was supported by a scholarship of the Studienstiftung des Deutschen Volkes. I. Jahreis was supported by a scholarship from the Konrad-Adenauer-Stiftung e.V.

References

Albano, C., et al., 2006. Successful treatment of epilepsy with serotonin reuptake inhibitors: proposed mechanism. Neurochemical Research 31, 509–514.
Aronica, E., et al., 2017. Neuroinflammatory targets and treatments for epilepsy validated in experimental models. Epilepsia 58 (Suppl. 3), 27–38.
Azmitia, E.C., et al., 1996. Cellular localization of the 5-HT1A receptor in primate brain neurons and glial cells. Neuropsychopharmacology 14, 35–46.
Bankstahl, M., et al., 2012. Inter-individual variation in the anticonvulsant effect of phenobarbital in the pilocarpine rat model of temporal lobe epilepsy. Exp. Neurol. 234, 70–84.
Bascuñana, P., et al., 2018. Divergent metabolic substrate utilization in brain during epileptogenesis precedes chronic hypometabolism. J Cereb Blood Flow Metab 271678X18809886.
Bascunana, P., et al., 2019a. PET neuroimaging reveals serotonergic and metabolic dysfunctions in the hippocampal electrical kindling model of epileptogenesis. Neuroscience 409, 101–110.
Bascunana, P., et al., 2019b. Ex vivo characterization of neuroinflammatory and neuroreceptor changes during epileptogenesis using candidate positron emission tomography biomarkers. Epilepsia 60, 2325–2333.
Bascuñana, P., et al., 2016. [(18)F]FDG PET neuroimaging predicts pentylenetetrazole (PTZ) kindling outcome in rats. Mol Imaging Biol 18, 733–740.
Bertoglio, D., et al., 2021. TSPO PET upregulation predicts epileptic phenotype at disease onset independently from chronic TSPO expression in a rat model of temporal lobe epilepsy. Neuroimage Clin 31, 102701.
Bertoglio, D., et al., 2017. Non-invasive PET imaging of brain inflammation at disease onset predicts spontaneous recurrent seizures and reflects comorbidities. Brain Behav. Immun. 61, 69–79.
Blazhenets, G., et al., 2019. Predictive value of (18)F-florbetapir and (18)F-FDG PET for conversion from mild cognitive impairment to alzheimer dementia. J. Nucl. Med.
Brackhan, M., et al., 2016. Serial quantitative TSPO-targeted PET reveals peak microglial activation up to 2 Weeks after an epileptogenic brain insult. J. Nucl. Med. 57, 1302–1308.
Breuer, H., et al., 2017. Multimodality imaging of blood-brain barrier impairment during epileptogenesis. J Cereb Blood Flow Metab 37, 2049–2061.
Bymaster, F.P., et al., 2002. Fluoxetine, but not other selective serotonin uptake inhibitors, increases norepinephrine and dopamine extracellular levels in prefrontal cortex. Psychopharmacology (Berl). 160, 353–361.

Caminiti, S.P., et al., 2018. FDG-PET and CSF biomarker accuracy in prediction of conversion to different dementias in a large multicentre MCI cohort. Neuroimage Clin 18, 167–177.
Chang, B.S., Lowenstein, D.H., 2003. Epilepsy. N Engl J Med. 349, 1257–1266.
Di Liberto, V., et al., 2018. Imaging correlates of behavioral impairments: an experimental PET study in the rat pilocarpine epilepsy model. Neurobiol. Dis. 118, 9–21.
Didelot, A., et al., 2008. PET imaging of brain 5-HT1A receptors in the preoperative evaluation of temporal lobe epilepsy. Brain : a journal of neurology 131, 2751–2764.
Engel Jr., J., et al., 2013. Epilepsy biomarkers. Epilepsia 54 (Suppl. 4), 61–69.
Garcia-Garcia, L., et al., 2017. Metyrapone prevents brain damage induced by status epilepticus in the rat lithium-pilocarpine model. Neuropharmacology 123, 261–273.
Goffin, K., et al., 2009. Longitudinal microPET imaging of brain glucose metabolism in rat lithium-pilocarpine model of epilepsy. Exp. Neurol. 217, 205–209.
Hernandez, E.J., et al., 2002. Effects of fluoxetine and TFMPP on spontaneous seizures in rats with pilocarpine-induced epilepsy. Epilepsia 43, 1337–1345.
Jahreis, I., et al., 2021. Choice of anesthesia and data analysis method strongly increases sensitivity of 18F-FDG PET imaging during experimental epileptogenesis. PLoS One 16, e0260482.
Johnston, A., et al., 2014. 5-Hydroxytryptamine1A receptor-activation hyperpolarizes pyramidal cells and suppresses hippocampal gamma oscillations via Kir3 channel activation. J Physiol. 592, 4187–4199.
Kessler, M., et al., 2019. GABAA receptors in the Mongolian gerbil: a PET study using [(18)F]flumazenil to determine receptor binding in young and old animals. Mol Imaging Biol.
Koch, S., et al., 2002. R-fluoxetine increases extracellular DA, NE, as well as 5-HT in rat prefrontal cortex and hypothalamus: an in vivo microdialysis and receptor binding study. Neuropsychopharmacology 27, 949–959.
Martín, E., Pozo, M., 2006. Animal models for the development of new neuropharmacological therapeutics in the status epilepticus. Curr. Neuropharmacol. 4, 33–40.
Mazarati, A., et al., 2008. Depression after status epilepticus: behavioural and biochemical deficits and effects of fluoxetine. Brain 131, 2071–2083.
Neveu, J., et al., 2021. Fluoxetine as adjunctive therapy in pediatric patients with refractory epilepsy: a retrospective analysis. Epilepsy Res. 177, 106780.
Paxinos, G., Watson, C., 2004. The rat brain in stereotaxic coordinates - the new coronal set. English 209.
Petry, F., et al., 2023. Fluoxetine and curcumin prevent the alterations in locomotor and exploratory activities and social interaction elicited by immunoinflammatory activation in zebrafish: involvement of BDNF and proinflammatory cytokines. ACS Chem. Neurosci. 14, 389–399.
Pitkanen, A., et al., 2016. Advances in the development of biomarkers for epilepsy. Lancet Neurol. 15, 843–856.
Pitkänen, A., Lukasiuk, K., 2011. Mechanisms of epileptogenesis and potential treatment targets. Lancet Neurol. 10, 173–186.
Pitkanen, A., et al., 2015. Epileptogenesis. Cold Spring Harb Perspect Med. 5.
Polascheck, N., et al., 2010. The COX-2 inhibitor parecoxib is neuroprotective but not antiepileptogenic in the pilocarpine model of temporal lobe epilepsy. Exp. Neurol. 224, 219–233.
Racine, R.J., 1972. Modification of seizure activity by electrical stimulation. II. Motor seizure. Electroencephalogr. Clin. Neurophysiol. 32, 281–294.
Russmann, V., et al., 2017. Identification of brain regions predicting epileptogenesis by serial [(18)F]GE-180 positron emission tomography imaging of neuroinflammation in a rat model of temporal lobe epilepsy. Neuroimage Clin 15, 35–44.
Schiffer, W.K., et al., 2006. Serial microPET measures of the metabolic reaction to a microdialysis probe implant. J. Neurosci. Methods 155, 272–284.
Schönhoff, K., et al., 2021. Hippocampal and septal 5-HT(1A) receptor expression in two rat models of temporal lobe epilepsy. Neuroscience 465, 219–230.
Shiha, A.A., et al., 2015. Subacute administration of fluoxetine prevents short-term brain hypometabolism and reduces brain damage markers induced by the lithium-pilocarpine model of epilepsy in rats. Brain Res. Bull. 111, 36–47.
Stahl, S.M., 1998. Basic psychopharmacology of antidepressants, part 1: antidepressants have seven distinct mechanisms of action. J. Clin. Psychiatry 59 (Suppl. 4), 5–14.
Stahl, S.M., 2015. Modes and nodes explain the mechanism of action of vortioxetine, a multimodal agent (MMA): blocking 5HT3 receptors enhances release of serotonin, norepinephrine, and acetylcholine. CNS Spectr. 20, 455–459.
Thackeray, J.T., et al., 2018. Myocardial inflammation predicts remodeling and neuroinflammation after myocardial infarction. J. Am. Coll. Cardiol. 71, 263–275.
Vezzani, A., et al., 2011. The role of inflammation in epilepsy. Nat. Rev. Neurol. 7, 31–40.
Vezzani, A., et al., 2013. The role of inflammation in epileptogenesis. Neuropharmacology 69, 16–24.
Watanabe, K., et al., 1998. Effect of acute administration of various 5-HT receptor agonists on focal hippocampal seizures in freely moving rats. Eur. J. Pharmacol. 350, 181–188.
Wolf, B.J., et al., 2020. TSPO PET identifies different anti-inflammatory minocycline treatment response in two rodent models of epileptogenesis. Neurotherapeutics 17, 1228–1238.
Yan, Q.S., et al., 1995. Further evidence of anticonvulsant role for 5-hydroxytryptamine in genetically epilepsy-prone rats. Br. J. Pharmacol. 115, 1314–1318.
Yao, Y., et al., 2023. Fluoxetine alleviates postoperative cognitive dysfunction by attenuating TLR4/MyD88/NF-κB signaling pathway activation in aged mice. Inflamm. Res. 72, 1161–1173.
Zhang, J., et al., 2022. Fluoxetine shows neuroprotective effects against LPS-induced neuroinflammation via the Notch signaling pathway. Int Immunopharmacol 113, 109417.
Zhang, L., et al., 2015. FDG-PET and NeuN-GFAP immunohistochemistry of hippocampus at different phases of the pilocarpine model of temporal lobe epilepsy. International journal of medical sciences 12, 288–294.